 FDMP, vol.11, no.3, pp.205-220, 2015

Numerical Simulation of Droplet Breakup, Splitting and Sorting in a Microfluidic Device

Chekifi. T[1,2], Dennai. B[1], Khelfaoui. R[1]

Abstract: Droplet generation, splitting and sorting are investigated numerically in the framework of a VOF technique for interface tracking and a finite-volume numerical method using the commercial code FLUENT. Droplets of water-in-oil are produced by a flow focusing technique relying on the use of a microchannell equipped with an obstacle to split the droplets. The influence of several parameters potentially affecting this process is investigated parametrically towards the end of identifying "optimal" conditions for droplet breakup. Such parameters include surface tension, the capillary number and the main channel width. We show that the capillary number plays a crucial role in determining droplet properties and the efficiency of the related generation process. An obstacle configuration can be effectively used to split a droplet, with the droplets being naturally sorted at the end of the main channel. Larger values of the capillary number generally lead to an increase in the droplet frequency and a decrease in its typical size.

Keywords: Water droplet; flow focusing; splitting; sorting; CFD; VOF and microchannel.

Nomenclature

f: frequency (Hz)

u: velocity (m/s)

u_c: continuous phase velocity (m/s)

u_d: dispersed phase velocity (m/s)

n: unit vector normal to the interface.

κ: curvature of the interface

[1] ENERGARID, Mechanical Engineering Department, University Tahri Mohamed Bechar, Bp. 417, route de Kenadsa, 08000 Bechar, Algeria.

[2] Corresponding Author. Tel.: +21349 815581/91, fax: +21349 815244; Email: chekifi.tawfiq@gmail.com

F: the surface tension force

W: width (mm)

ρ: density (kg/m^3)

μ: dynamic viscosity (kg/m^{-1}·s^{-1})

α: phase fraction (%)

σ: the surface tension coefficient (N/m)

τ: time (s)

W: width of the main channel

W_c: width of continuous phase inlet

W_d: width of continuous phase inlet

ρ_c: continuous phase density

ρ_d: dispersed phase density

1 Introduction

Over the last few decades, modeling of immiscible fluids such as oil and water has become a classical research topic. Droplet-based microfluidics can be regarded as a unique platform for techniques related to mixing, reaction, separation, dispersion of drops and numerous other applications [Burns, Mastrangelo, Sammarco, Man, Webster, Johnsons, Foerster, Jones, Fields, Kaiser, et al. (1996); Lehmann, Hadjidj, Parashar, Vandevyver, Rida, and Gijs (2006)]. Droplet-based microfluidics is a subject of great interest for biological research, chemical synthesis, drug delivery and medical diagnostics.

It refers to devices and methods for controlling fluid flow at length scales smaller than one millimeter. Monodisperse droplets in microfluidic devices have been generated using different microchannel configurations such as T-junctions [Garstecki, Fuerstman, Stone, and Whitesides (2006a); Xu, Li, Tan,Wang, and Luo (2006)], flow focusing [Nguyen, Ting, Yap, Wong, Chai, Ong, Zhou, Tan, and Yobas (2007)], or co-flowing [Xu, Li, Lan, and Luo (2008)]. In microfluidics, controlling droplet size is a central issue not only for producing monodisperse emulsions [Chu, Utada, Shah, Kim, and Weitz (2007)], but also for using the droplet itself as a tool for manifold purposes [Teh, Lin, Hung, and Lee (2008); Whitesides (2006)].

With regard to droplet breakup, Link et al. (2004) introduced two methods to reduce droplet size using T-junctions or a square obstruction located in the center of the channel [Link, Anna, Weitz, and Stone (2004)]. As these methods are "passive", they provide a way of reducing droplet size in a rapid process with a narrow size distribution.

In recent studies, unlike relatively simple geometries such as T-junctions [Thorsen, Roberts, Arnold, and Quake (2001); Priest, Herminghaus, and Seemann (2006)] or flow focusing devices [Anna, Bontoux, and Stone (2003a); Anna and Mayer (2006)], novel designs have been developed for improved manipulation of droplets. Lee, Lin, and Lee (2009) presented a one-step method for size control and sorting of droplets in a modified flow focusing geometry with a moving wall technique operated by pressure inlets. Also, in a cross-shaped channel, droplet generation by a thread breakup due to pressure inlets at both sides was shown with a surface treatment technique [Su and Lin (2006)]. Droplet fusion devices were also proposed using a hydrodynamic trap at a wide cross channel [Tan, Ho, and Lee (2007); Tan, Fisher, Lee, Cristini, and Lee (2004)], at a tapered channel [Hung, Choi, Tseng, Tan, Shea, and Lee (2006)], at a fluid resistance in straight channels [Köhler, Henkel, Grodrian, Kirner, Roth, Martin, and Metze (2004)], and an array of pillar elements [Niu, Gulati, Edel, et al. (2008)]. As mentioned previously, an obstruction in microchannel can also be utilized to reduce the droplet size [Link, Anna, Weitz, and Stone (2004)]. [De Menech (2006)] was performed numerical analysis to figure out the droplet breakup process and optimize the geometry configuration for the process. In which, the author suggested T-junction channel using a phase-field method to compute droplet breakup, Carlson, Do-Quang, and Amberg (2010) extended the phase field method to simulation of droplet motion in a Y-junction channel. Their results showed that the tip of the junction affected the droplet deformation, and the droplet breakup or non-breakup regime depended on the capillary number and droplet size. The droplet breakup by a circular cylinder in a microchannel was computed by Chung, Lee, Char, Ahn, and Lee (2010) using a front tracking method, in which the droplet shape was represented by the moving front elements. Their numerical results showed that the split droplets merged in the rear side of the obstacle when the capillary number was not large.

Although various studies on the generation of droplets in T-junction and flow focusing devices have been carried out, a fundamental understanding of the flow physics that account for the effect of the geometry of the devices is still missing. In addition, simulation of two immiscible phases flow in complex geometry is a challenging work [Shi, Tang, and Xia (2014)].

Computational fluid dynamics (CFD) studies allow for broad parametric variations that are hard to study experimentally. CFD also provides detailed information on flow details such as pressures and velocities that are difficult to measure experimentally, and can thus provide mechanistic insights needed to check various hypotheses. Recently, the volume of fluids method has been proved to be a powerful method to simulate droplet dynamics [Nichita, Zun, and Thome (2010)]. In this method, the interface is given implicitly by a color function, which is defined

as the volume fraction of one of the fluids within each cell. From this function, a reconstruction of the interface is made and the interface is then propagated implicitly by updating the color function. VOF methods are conservative and can deal with topological changes of the interface. However, VOF methods cannot accurately compute several important properties, such as curvature and the normal to the interface. Moreover, a high order of accuracy is hard to achieve because of the discontinuities in the color function [Nichita, Zun, and Thome (2010)].

Motivated by the previous work [Shi, Tang, and Xia (2014)] and [Lee, Lee, and Son (2013)], using a VOF method, we perform a two-dimensional numerical CFD study of droplet breakup, splitting and sorting, in the present study we suggest device that allows droplet breakup in flow focusing configuration, splitting and sorting. In this microsystem, the effect of main channel size and capillary number on the droplet dynamics is investigated. In previous numerical works [Nichita, Zun, and Thome (2010); Duong, Luis, Portela, and Chris], surface tension plays a significant role on the droplet deformation in confined microchannel flows. In the same manner, by testing a several values between both phases, we expect that this parameter affects the droplet dispersion in the microchannel. In which, the effects of inertia and gravity in the volume does not play an important role with respect to the macroscopic scale. we also study the droplet breakup as function of the capillary number and the main channel size to find the optimal conditions for droplet detachment. In our model, we investigate the droplet splitting and sorting by size in the end of the main channel by the use of an obstacle. The frequency of droplet generation and droplet sorting is also considered. Finally, we suggest useful ideas for manipulating droplets in microchannel flows.

2 Description of the system and geometries

The physics to be simulated involves droplet breakup by flow focusing technique. Three sizes of the main channel are evaluated to produce water-in-oil droplet. There are two oil inlets, one water inlet and one outlet in. All the micro- channels are 5 mm long. The description of the geometries is presented in Fig. 1. Due to the existence of the obstacle, two sub-channels are formed in the end of main channel.

In our system, the droplet are generated by the flow focusing, which has been widely used for generating highly spherical droplet [Anna, Bontoux, and Stone (2003b); Zhao and Middelberg (2011); Hamlington, Steinhaus, Feng, Link, Shelley, and Shen (2007)]. Fig. 1 shows the flow focusing geometry implemented into a microfluidic device. In this structure, the dispersed phase flows in the middle of the channel, while the continuous phase flows through upper and lower channels. The continuous phase and dispersed phase penetrate into the downstream channel, and the continuous phase exerts pressure and stress which force the dispersed phase in-

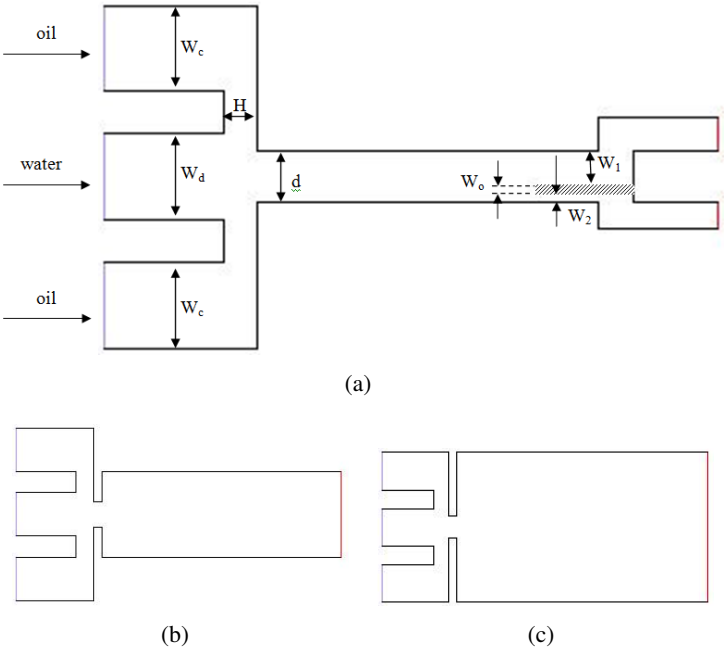

Figure 1: (a): Schematic of flow focusing configuration. $W_c = W_d = 2$. An orifice with width $d = 1.2$ is placed at a distance $H = 0.8$ downstream of three coaxial streams. The main channel width is varied (a): $W = 1.2$, (b): $W = 4$ and (c): $W = 8$). $W_o = 0.16$, sub-channel 1: $W_1 = 0.8$, sub-channel 2: $W_2 = 0.24$. The total length of the configuration is 12. (All the numbers are in mm).

to a narrow thread. The dispersed phase breaks inside or downstream of the orifice, then the droplet is generated at the end of the flow stream where the neck forms.

The surface tension term reflects the interfacial force between the discrete liquid (droplet) and the continuous liquid. The interaction (attraction or repulsion) between droplets results from the continuous liquid flow which is affected by the interfacial forces existing at each droplet surface.

3 Numerical approach

The segregated solver for an unsteady laminar flow was used in CFD, the volume of fluid method was performed to track the interface between water droplet and the continuous phase. The VOF model is a surface-tracking technique that is useful when studying the position of the interface between two immiscible fluids. A single set of momentum equations is shared by the fluids, and the volume fraction of each

of the fluids in each computational cell is tracked throughout the domain. The VOF model uses phase averaging to define the amount of continuous and dispersed phase in each cell. A variable, α, was defined as Timgren, Trägårdh, and Trägårdh (2007):

$\alpha = 1 \Rightarrow$ when the cell is 100% filled with continuous phase

$\alpha = 0 \Rightarrow$ when the cell is 100% filled with dispersed phase

$0 < \alpha < 1 \Rightarrow$ when the cell contains an interface between the two phases.

The density ρ, and viscosity μ, for both phases (water and oil) can be calculated using a linear dependence:

The subscript 1 is chosen for the continuous liquid (primary) phase, while the subscript 2 for the discrete phase (microdrops)

$$\rho = \rho_1 \alpha + \rho_2 (1 - \alpha) \tag{1}$$

$$\mu = \mu_1 \alpha + \mu_2 (1 - \alpha) \tag{2}$$

There are several different VOF algorithms with different accuracies and complexities in CFD. The geometric reconstruction scheme used in this study is based on the work of Youngs (1982) and further described by Rudman (1997). This scheme permits a piecewise-linear approach, which assumes that the interface has a linear slope within each cell, and the position of the interface is calculated from the volume fraction and their derivatives in the cell. The solutions of the velocity field and pressure are calculated using a body-force-weighted discretization scheme for the pressure, the Pressure-Implicit with Splitting of Operators (PISO) scheme for the pressure velocity.

The body-force-weighted scheme is used since it works well with the VOF model, and the PISO scheme is chosen to improve the efficiency of the calculation of the momentum balance after the pressure correction equation is solved.

The CFD software was used to simulate the flow of oil microdrops sorting. The governing equations are the mass conservation equation for each phase and the momentum equation:

$$\partial_t C + \vec{u} \nabla C = 0 \tag{3}$$

where the velocity is given by u. In addition, a single momentum equation is used for the mixture of two-phase-fluid.

The momentum equation hence is described by:

$$\frac{\partial}{\partial_t}(\rho u) + \nabla \cdot (\rho u u) + \nabla u \cdot \nabla [\nu] = -\nabla P + F \tag{4}$$

Where F is the surface tension force $F = \rho(x)n$ is the curvature of the interface and n is a unit vector normal to the interface. σ is the surface tension coefficient.

4 Droplet simulation and parameters

FLUENT 6.3 in CFD software was used to model droplet formation in the microfluidic by flow focusing configuration (see Fig. 1). The volume of fluid (VOF) model in three-dimensional form was used, which enables capturing and tracking the precise location of the interface between the fluids. The VOF method operates under the principle that the two or more fluids are not interpenetrating. The flows are taken to be two-dimensional and laminar. In the simulations, a constant velocity boundary scheme proposed by Zou and He (1997) is imposed on both water and oil inlet and the pressure of outlet is the same as the atmospheric pressure. At the position where the fluid meets the solid walls, half-way bounce-back boundary scheme is applied to achieve the non-slip velocity condition at the solid walls. The viscosities of both liquids water and gasoil are respectively defined as $\mu_w = 0.001$ kg/m.s^{-1}, $\mu_o = 0.003$ kg/m.s^{-1}. An equilibrium contact angle $\theta = 60^\circ$ were prescribed. This contact angle is used to correct the surface normal in the vicinity of the wall, and therefore adjusts the curvature of the interface and the surface tension calculation near the wall [Duong, Luis, Portela, and Chris]. The second-order upwind scheme is used for discretization of the momentum equation. The PISO scheme is taken as the pressure-velocity coupling scheme, while the PRESTO! is taken as the pressure discretization scheme. The geometric reconstruction scheme is used for interpolation of the interface geometry. It is able to form mono-dispersed droplets by this way due to the different surface tensions of two fluids.

The computations were run for a large number of time steps (10^{-5}) to generate a database from which statistically converged mean and perturbation flow quantities could be extracted. The convergence limit was set to a residual sum of 10^{-3} for the continuity and velocity components. These results are discussed in the following sections.

The requirement to successfully follow of droplets behavior leads to very large numbers of grid cells when uniform meshes are used. Three intervals mesh sizes were tested to obtain grid independent solutions ($h = 0.06$, $h = 0.08$ and $h = 0.1$ μm). The relative difference of droplet volumes and interface shapes between successive mesh sizes is observed to be small as the mesh size decreases. Therefore, our simulations in this study are done with $h = 1$ μm to save computing time without losing the accuracy of the numerical results.

4.1 The main channel width effects

To test whether the confinement of geometry plays an important role in the breakup of plugs, [Garstecki, Fuerstman, Stone, and Whitesides (2006b); Christopher, Noharuddin, Taylor, and Anna (2008); Xu, Li, Tan, and Luo (2008)] we first perform computations to investigate the effect of the main channel width on the droplet flow regime. In the simulations, to single out the geometrical parameter, the inlet flow velocity of both phases is ($u_d = u_c = 0.2$m/s), the densities of both fluids are $\rho_c =$ 830m^3/kg and $\rho_d = 998.2$ m^3/kg. the results for three configuration are presented in the fig. 2.

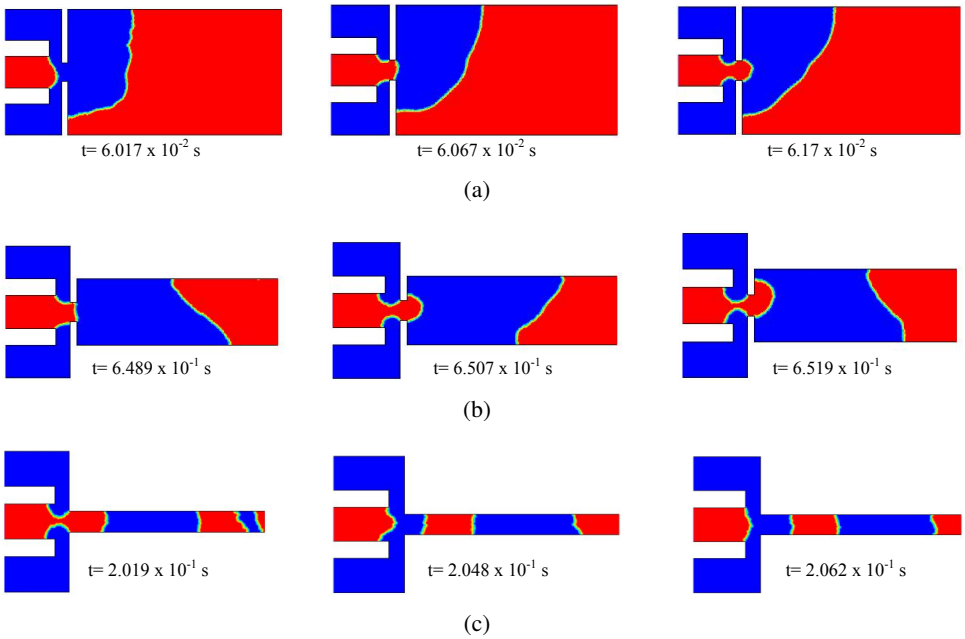

Figure 2: The droplet generation at $u_d/u_c = 1$ ($u_d = u_c = 0.2$m/s) for three different widths of main channel. (a) $W = 8$mm. b) $W = 4$ mm and c) $W = 1.2$ mm.

The geometry effect, i.e., the width of the main channel (W) plays an important role in the flow dispersion in the main channel Fig. 2, at the same conditions for large main channel the flow is observed in thread regime due to the accumulation of generated droplets, which are flew with low velocity fig.2 a) and b), where droplet emerging is occurred. For the smallest model Fig.2 c), no emerging is observed, because droplets flow with high velocities. Therefore, the flow pattern is clearly observed with high dispersion. For the next sections, we use the smallest model with main channel width = 1.2.

4.2 Surface tension effect

For two phase flows in microchannels, the surface tension forces play an important role in determining the dynamics of droplets, whereas gravitational forces are generally less important, we investigate the influence of surface tension coefficient on the droplet flow regime.

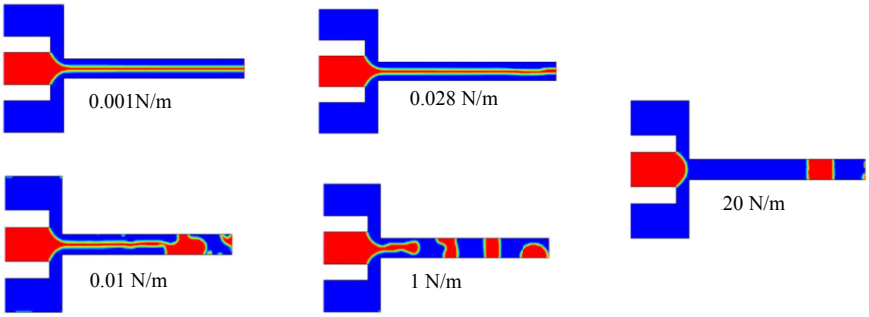

Figure 3: Droplet flow regimes as a function of the surface tension (σ) for $u_c/u_d = 1$ ($u_c = u_d = 0.2$m/s) for the small model.

In this subsection, we use water as the dispersed phase and oil as the continuous phase, and observe flow regime, which depends on the surface tension coefficient. The densities of the continuous and dispersed phase are assumed respectively $\rho_c = 830\text{m}^3/\text{kg}$ and $\rho_d = 998.2\ \text{m}^3/\text{kg}$. The channel surface is hydrophobic, i.e., the contact angle between dispersed phase and the channel surface is $\theta = 0^\circ$. It is shown in Fig. 3 that for Capillary numbers which define flows in the jetting to dripping regime through numerical simulations, and quantify the results in terms of the "stable" droplet formation regime in a microchannel. for a given inlet velocity of both phases ($u = 0.2$) As shown in Fig. 3, three typical flow patterns are identified for different surface tension at a fixed capillary number (Ca = 3.43 x 10^{-2}). For low σ, thread regime of dispersed phase is clearly observed, as we increase σ, the thread becomes unstable after a distance of laminar flow $\sigma = 0.01$ N/m, for higher surface tension $\sigma = 20$ N/m, droplet are formed with high dispersion due to the squeezing mechanism. For the next simulations, we use $\sigma = 20$N/m to generate mono dispersed droplet.

4.3 Contact angle effect

Wetting properties are usually characterized by the contact angle on a surface. Young's law provides the relation between interfacial tensions and contact angle. For a water droplet on a surface, surrounded by oil, the equilibrium contact angle

is [Liu, Valocchi, and Kang (2010)].

$$\cos(\theta) = \frac{\sigma_{oil,wall} - \sigma_{water,wall}}{\sigma_{oil,water}}$$

Where $\sigma_{oil,wall}$ is the interfacial tension of oil with the wall surface, rwater, wall is the interfacial tension of water with the wall surface, and $\sigma_{oil,water}$ is the interfacial tension of the oil with water interface.

A constant contact angle associated to a non slip condition was imposed at the contact point between the gas–liquid interface and the walls defining our structure. The corresponding numerical procedure is described in detail in Dupont and Legendre [Hung, Choi, Tseng, Tan, Shea, and Lee (2006)]. The result of the droplet flow pattern as function of contact angle is presented in the fig. 4.

The wetting properties of the fluids relative to the channel walls, more specifically the contact angle, have also been shown to affect the two-phase flow patterns in microchannels [Rosengarten, Harvie, and Cooper-White (2006)]. In order to determine the influence of the contact angles on droplet shape, different values of the contact angles ($\Theta = 0^\circ$, $\Theta = 60^\circ$, $\Theta = 90^\circ$, $\Theta = 120^\circ$ and $\Theta = 180^\circ$) are tested by keeping the same conditions to find the optimum contact angle to obtain spherical form of droplet. It is clearly observed that the droplet takes a shape for each contact angle. For $\Theta = 0^\circ$, elongated droplet are observed with low production frequency, whereas the rest of contact angle the geometrical form is smaller. For $\Theta = 90^\circ$, the droplet takes uniform rectangular shape with high production frequency compared of $\Theta = 0^\circ$. For both $\Theta = 120^\circ$ and $\Theta = 180^\circ$ droplets take concaved shape in its extremity. The contact angle of 60° is the optimum condition for droplet flow pattern; which is used for the next sections. In this contact angle the droplet are taken uniform spherical shape.

5 Droplet splitting and sorting

Numerical simulations of droplet breakup and splitting are performed using VOF method, droplet of water-in-oil are generated by flow focusing configuration, The simplest droplet sorting techniques require no detection or switching mechanisms, but instead rely on creative device geometry that allows the separation of droplets by size. By simply creating an obstacle geometry in which the daughter channels had different widths, droplets were induced to sort into one of the channels (Fig. 5). The split daughter droplets pass the sub-channels, while the bigger split daughter droplets pass the sub-channels 2. When a droplet collides with the obstacle, it splits into the obstacle-wall gaps (or sub-channels). The split portions of droplet leave out the sub-channels to the outlet of microsystem.

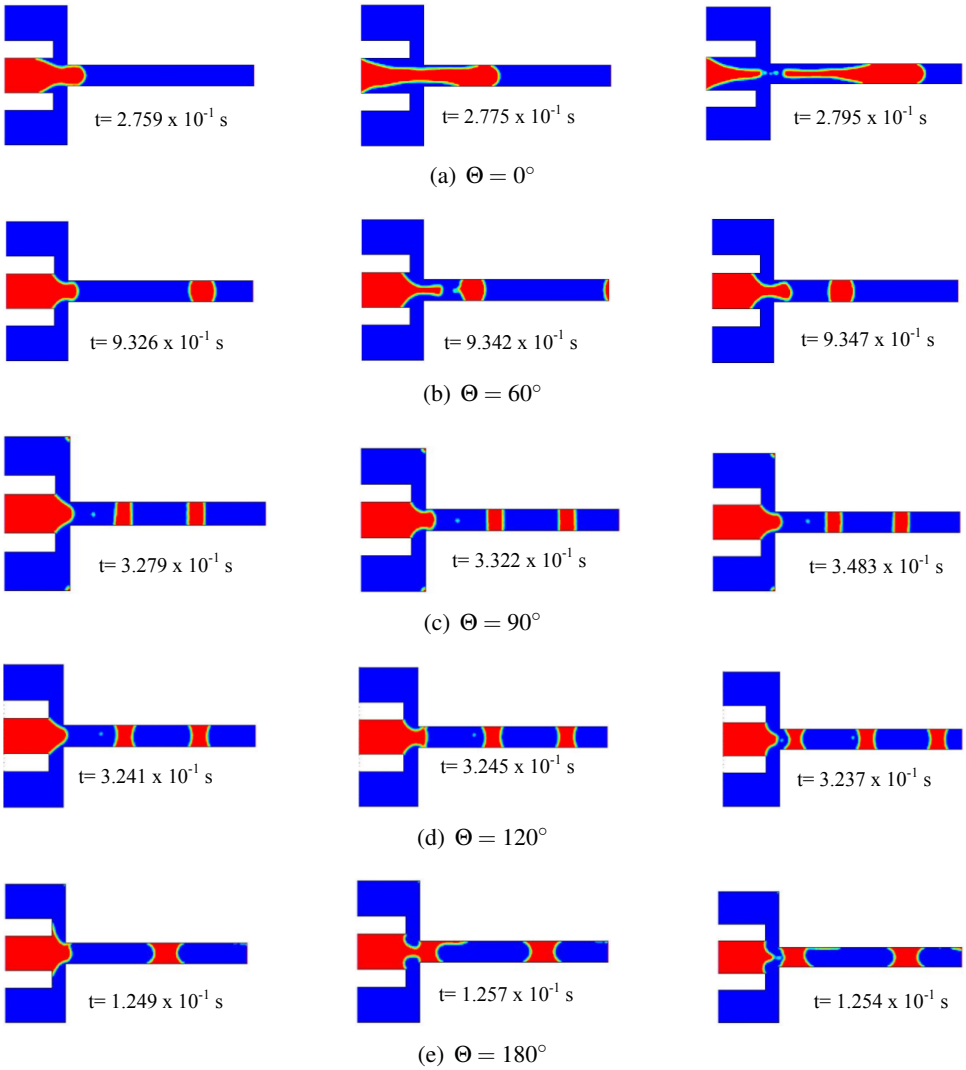

Figure 4: Droplet (water-in-oil) flow pattern as a function of contact angle at Ca = 0.053 ($u_c = 0.5$m/s and $u_d = 0.3$ m/s) and $\sigma = 10$ N/m.

Fig. 5 shows the droplet motion A convergence test for grid resolutions is first conducted for droplet breakup by the use of a quadrate obstacle. Water-in-oil droplet are generated by flow focusing configuration, splitting of droplet is performed by thinner obstacle at the end of the main channel, for both capillary numbers (Ca = 5.36 x 10^{-2} Ca = 6.64 x 10^{-2}). We observe for in three successive moments that the split daughter droplets pass the sub-channels without re-merging unlike; our

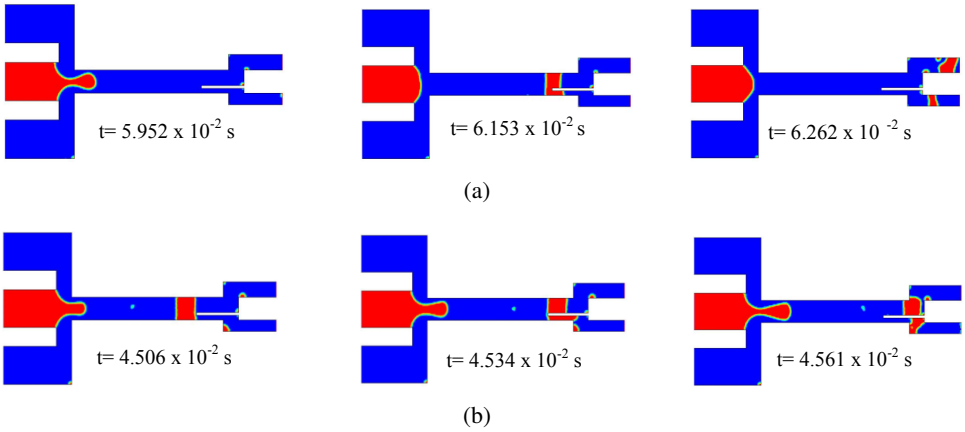

Figure 5: Droplet breakup, splitting and sorting for two different capillary numbers: a) $u_c = 1$m/s, $u_d = 0.1$ m/s Ca $= 5.36$ x 10^{-2} and b) $u_c = 0.5$m/, $u_d = 0.3$ m/s Ca $= 6.64$ x 10^{-2}.

numerical simulations are in good agreement with previous works of [Lehmann, Hadjidj, Parashar, Vandevyver, Rida, and Gijs (2006)] and [Lee and Son (2013)]. It is also seen from Fig. 5 (b) that the droplet volume fraction is higher for higher capillary number fig 4. b), as we demonstrated in the previous section. Due to difference of both sub-channel widths, the bigger split daughter droplets pass the sub-channels 1, while the smaller split daughter droplets pass the sub-channels 2.

The present computations demonstrate that an inclined obstacle can be used as an effective method for droplet splitting with even-sized daughter droplets.

6 Conclusions

Droplet generation in flow focusing configuration, splitting and sorting were investigated numerically by using the VOF method of the commercial code FLUENT. Various parameters which affect the generation of the droplets, including capillary number, geometry of configuration, surface tension and contact angle are systematically analyzed. It shows that the droplet breakup depends on fluid properties such as capillary number, surface tension and the main channel width. We also find that the flow focusing configuration with the smaller main channel width likely to generate stable droplet. The capillary number is an important parameter to define the droplet length and droplet generation frequency. The increase of this parameter leads to the increase of droplet frequency, while it conducts to small droplet length. The numerical simulations of droplet breakup also showed that the obstacle configuration is effective for droplet splitting and sorting, where, daughter split droplet

are sorted into smaller droplet that passed through small sub-channel and the bigger passed the bigger sub-channel.

We hope this numerical study helps understanding the underlying physics on the droplet dynamics as well as designing the complicated flows in future microfluidic applications.

Acknowledgement: The authors wish to acknowledge ENERGARID laboratory, especially the group of integral system control.

References

Anna, S. L.; Bontoux, N.; Stone, H. A. (2003): Formation of dispersions using "flow focusing" in microchannels. *Applied physics letters*, vol. 82, no. 3, pp. 364–366.

Anna, S. L.; Bontoux, N.; Stone, H. A. (2003): Formation of dispersions using "flow focusing" in microchannels. *Applied physics letters*, vol. 82, no. 3, pp. 364–366.

Anna, S. L.; Mayer, H. C. (2006): Microscale tipstreaming in a microfluidic flow focusing device. *Physics of Fluids (1994-present)*, vol. 18, no. 12, pp. 121512.

Burns, M. A.; Mastrangelo, C. H.; Sammarco, T. S.; Man, F. P.; Webster, J. R.; Johnsons, B.; Foerster, B.; Jones, D.; Fields, Y.; Kaiser, A. R. et al. (1996): Microfabricated structures for integrated dna analysis. *Proceedings of the National Academy of Sciences*, vol. 93, no. 11, pp. 5556–5561.

Carlson, A.; Do-Quang, M.; Amberg, G. (2010): Droplet dynamics in a bifurcating channel. *International Journal of Multiphase Flow*, vol. 36, no. 5, pp. 397–405.

Christopher, G. F.; Noharuddin, N. N.; Taylor, J. A.; Anna, S. L. (2008): Experimental observations of the squeezing-to-dripping transition in t-shaped microfluidic junctions. *Physical Review E*, vol. 78, no. 3, pp. 036317.

Chu, L.-Y.; Utada, A. S.; Shah, R. K.; Kim, J.-W.; Weitz, D. A. (2007): Controllable monodisperse multiple emulsions. *Angewandte Chemie International Edition*, vol. 46, no. 47, pp. 8970–8974.

Chung, C.; Ahn, K. H.; Lee, S. J. (2009): Numerical study on the dynamics of droplet passing through a cylinder obstruction in confined microchannel flow. *Journal of Non-Newtonian Fluid Mechanics*, vol. 162, no. 1, pp. 38–44.

Chung, C.; Lee, M.; Char, K.; Ahn, K. H.; Lee, S. J. (2010): Droplet dynamics passing through obstructions in confined microchannel flow. *Microfluidics and nanofluidics*, vol. 9, no. 6, pp. 1151–1163.

De Menech, M. (2006): Modeling of droplet breakup in a microfluidic t-shaped junction with a phase-field model. *Physical Review E*, vol. 73, no. 3, pp. 031505.

Garstecki, P.; Fuerstman, M. J.; Stone, H. A.; Whitesides, G. M. (2006): Formation of droplets and bubbles in a microfluidic t-junction–scaling and mechanism of break-up. *Lab on a Chip*, vol. 6, no. 3, pp. 437–446.

Garstecki, P.; Fuerstman, M. J.; Stone, H. A.; Whitesides, G. M. (2006): Formation of droplets and bubbles in a microfluidic t-junction–scaling and mechanism of break-up. *Lab on a Chip*, vol. 6, no. 3, pp. 437–446.

Hamlington, B. D.; Steinhaus, B.; Feng, J. J.; Link, D.; Shelley, M. J.; Shen, A. Q. (2007): Liquid crystal droplet production in a microfluidic device. *Liquid Crystals*, vol. 34, no. 7, pp. 861–870.

Duong A. Hoang, Luis M. Portela, Chris R. Kleijn, Numerical study on droplet breakup in a microfluidic t-junction.

Hung, L.-H.; Choi, K. M.; Tseng, W.-Y.; Tan, Y.-C.; Shea, K. J.; Lee, A. P. (2006): Alternating droplet generation and controlled dynamic droplet fusion in microfluidic device for cds nanoparticle synthesis. *Lab on a Chip*, vol. 6, no. 2, pp. 174–178.

Köhler, J.; Henkel, T.; Grodrian, A.; Kirner, T.; Roth, M.; Martin, K.; Metze, J. (2004): Digital reaction technology by micro segmented flow–components, concepts and applications. *Chemical Engineering Journal*, vol. 101, no. 1, pp. 201–216.

Lee, C.-Y.; Lin, Y.-H.; Lee, G.-B. (2009): A droplet-based microfluidic system capable of droplet formation and manipulation. *Microfluidics and nanofluidics*, vol. 6, no. 5, pp. 599–610.

Lee, J.; Lee, W.; Son, G. (2013): Numerical study of droplet breakup and merging in a microfluidic channel. *Journal of Mechanical Science and Technology*, vol. 27, no. 6, pp. 1693–1699.

Lee, W.; Son, G. (2013): Numerical study of obstacle configuration for droplet splitting in a microchannel. *Computers & Fluids*, vol. 84, pp. 351–358.

Lehmann, U.; Hadjidj, S.; Parashar, V. K.; Vandevyver, C.; Rida, A.; Gijs, M. A. (2006): Two-dimensional magnetic manipulation of microdroplets on a chip as a platform for bioanalytical applications. *Sensors and Actuators B: Chemical*, vol. 117, no. 2, pp. 457–463.

Link, D.; Anna, S. L.; Weitz, D.; Stone, H. (2004): Geometrically mediated breakup of drops in microfluidic devices. *Physical review letters*, vol. 92, no. 5, pp. 054503.

Liu, H.; Valocchi, A. J.; Kang, Q. (2010): Pore-scale simulation of high-density-ratio multiphase flows in porous media using lattice boltzmann method. *Comput Phys*, vol. 229, pp. 8045–63.

Nguyen, N.-T.; Ting, T.-H.; Yap, Y.-F.; Wong, T.-N.; Chai, J. C.-K.; Ong, W.-L.; Zhou, J.; Tan, S.-H.; Yobas, L. (2007): Thermally mediated droplet formation in microchannels. *Applied Physics Letters*, vol. 91, no. 8, pp. 084102.

Nichita, B. A.; Zun, I.; Thome, J. R. (2010): A vof method coupled with a dynamic contact angle model for simulation of two-phase flows with partial wetting. In *7th International Conference on Multiphase Flow, ICMF 2010, Tampa, FL, May 30–June 4, 2010*, no. EPFL-CONF-150243.

Niu, X.; Gulati, S.; Edel, J. B. et al. (2008): Pillar-induced droplet merging in microfluidic circuits. *Lab on a chip*, vol. 8, no. 11, pp. 1837–1841.

Priest, C.; Herminghaus, S.; Seemann, R. (2006): Generation of monodisperse gel emulsions in a microfluidic device. *Applied physics letters*, vol. 88, no. 2, pp. 024106.

Rosengarten, G.; Harvie, D.; Cooper-White, J. (2006): Contact angle effects on microdroplet deformation using cfd. *Applied Mathematical Modelling*, vol. 30, no. 10, pp. 1033–1042.

Rudman, M. (1997): Volume-tracking methods for interfacial flow calculations. *International journal for numerical methods in fluids*, vol. 24, no. 7, pp. 671–691.

Shi, Y.; Tang, G.; Xia, H. (2014): Lattice boltzmann simulation of droplet formation in t-junction and flow focusing devices. *Computers & Fluids*, vol. 90, pp. 155–163.

Su, Y.-C.; Lin, L. (2006): Geometry and surface-assisted micro flow discretization. *Journal of Micromechanics and Microengineering*, vol. 16, no. 9, pp. 1884.

Tan, Y.-C.; Fisher, J. S.; Lee, A. I.; Cristini, V.; Lee, A. P. (2004): Design of microfluidic channel geometries for the control of droplet volume, chemical concentration, and sorting. *Lab on a Chip*, vol. 4, no. 4, pp. 292–298.

Tan, Y.-C.; Ho, Y. L.; Lee, A. P. (2007): Droplet coalescence by geometrically mediated flow in microfluidic channels. *Microfluidics and Nanofluidics*, vol. 3, no. 4, pp. 495–499.

Teh, S.-Y.; Lin, R.; Hung, L.-H.; Lee, A. P. (2008): Droplet microfluidics. *Lab on a Chip*, vol. 8, no. 2, pp. 198–220.

Thorsen, T.; Roberts, R. W.; Arnold, F. H.; Quake, S. R. (2001): Dynamic pattern formation in a vesicle-generating microfluidic device. *Physical review letters*, vol. 86, no. 18, pp. 4163.

Timgren, A.; Trägårdh, G.; Trägårdh, C. (2007): Cfd modelling of drop formation in a liquid-liquid system. In *6th International Conference on Multiphase Flow*, pp. 1–8. 6th International Conference on Multiphase Flow.

Whitesides, G. M. (2006): The origins and the future of microfluidics. *Nature*, vol. 442, no. 7101, pp. 368–373.

Xu, J.; Li, S.; Lan, W.; Luo, G. (2008): Microfluidic approach for rapid interfacial tension measurement. *Langmuir*, vol. 24, no. 19, pp. 11287–11292.

Xu, J.; Li, S.; Tan, J.; Luo, G. (2008): Correlations of droplet formation in t-junction microfluidic devices: from squeezing to dripping. *Microfluidics and Nanofluidics*, vol. 5, no. 6, pp. 711–717.

Xu, J.; Li, S.; Tan, J.; Wang, Y.; Luo, G. (2006): Preparation of highly monodisperse droplet in a t-junction microfluidic device. *AIChE journal*, vol. 52, no. 9, pp. 3005–3010.

Youngs, D. L. (1982): Time-dependent multi-material flow with large fluid distortion. *Numerical methods for fluid dynamics*, vol. 24, pp. 273–285.

Zhao, C.-X.; Middelberg, A. P. (2011): Two-phase microfluidic flows. *Chemical Engineering Science*, vol. 66, no. 7, pp. 1394–1411.

Zou, Q.; He, X. (1997): On pressure and velocity boundary conditions for the lattice boltzmann bgk model. *Physics of Fluids (1994-present)*, vol. 9, no. 6, pp. 1591–1598.